Pergamon

Int. J. Heat Mass Transfer. Vol. 38, No. 9, pp. 1719–1731, 1995

0017 9310/95 $9.50+0.00

0017–9310(94)00275–4

Mass transfer enhancement in a symmetric sinusoidal wavy-walled channel for pulsatile flow

TATSUO NISHIMURA and NAOYA KOJIMA

Department of Mechanical Engineering, Yamaguchi University, Ube 755, Japan

(*Received* 17 *March* 1994 *and in final form* 16 *June* 1994)

Abstract—Mass transfer characteristics in a sinusoidal wavy-walled channel are investigated experimentally for pulsatile flow with varying flow parameters, i.e. net flow, amplitude and frequency of fluid oscillation. We show that combination of flow separation and fluid oscillation leads to a significant enhancement in the mass transfer rate under laminar flow conditions. This enhancement is due to rapid fluid mixing induced by the dynamic behavior of the vortex in this channel. The Sherwood number for pulsatile flow can be expressed by the following relation:

$$Sh_p^m = Sh_s^m + Sh_o^m$$

where m is the exponent, and subscripts mean s—steady flow, o—oscillatory flow and p—pulsatile flow. Although the value of m depends on the amplitude of fluid oscillation, it becomes constant at large amplitude, i.e. $m = 4$.

1. INTRODUCTION

Heat and mass transfer enhancement for laminar flow has recently assumed great importance in the fields of medical and biochemical engineering. For example, when blood oxygenators and bioreactors process very viscous liquids containing shear-sensitive biomaterials such as animal cells and plant cells, it is necessary to use laminar flow rather than rely on turbulence to obtain efficient mixing and excellent heat and mass transfer characteristics.

A broad range of enhancement schemes for heat and mass transfer are used in everyday engineering practice. For single-phase systems we can identify two methods:

(1) decreasing resistance in the restarting thermal and compositional boundary layers;

(2) increasing mixing by improving exchange of fluid normal to the heat and mass transfer surfaces.

An important group of methods of the second category involves mixing produced by unsteady flows. Ottino [1] studied fluid mixing by chaotic advection, in which fluid elements follow irregular paths in regular velocity fields. Chaotic advection has been observed for a wide range of unsteady flows. Aref [2] and other investigators have observed chaotic advective motion for simple time-periodic two-dimensional flow, leading to rapid mixing. This suggests a very interesting and exciting application, by which enhanced heat and mass transfer can be achieved with a regular laminar flow. However, few studies have been performed on heat and mass transfer enhancement by time-periodic flows.

Bellhouse *et al.* [3] pioneered the study of how large fluid oscillations can improve fluid mixing and mass transfer in a furrowed channel and applied this scheme to a high-efficiency membrane oxygenator. Subsequently, Patera and Mikic [4] and Greiner [5] found that small fluid oscillations at the natural frequency of the hydrodynamic instability dramatically increase the amplitude of the instability within a grooved channel, even for Reynolds numbers below the critical value at the onset of self-sustained oscillations, and thus enhance heat transfer. They called this resonant enhancement. Mackley *et al.* [6] and Mackley and Ni [7] studied experimentally the effect of fluid oscillation within a baffled tube, and showed that excellent fluid mixing and heat transfer can be achieved. Furthermore, Howes *et al.* [8] indicated numerically that chaotic advection is observed in a baffled channel for unsteady flows. These studies demonstrated that rapid fluid mixing, which is induced by the use of fluid oscillation superimposed on a net flow, can enhance heat and mass transfer in some industrial devices. However, it is not known how flow parameters influence heat and mass transfer enhancement. That is, their experiments deal with the effect of the frequency of fluid oscillation, but the effects of net flow and the amplitude of oscillation have not been explored.

For oscillatory flow without a net flow, Nishimura *et al.* [9–12] studied flow and mass transfer characteristics in sinusoidal wavy-walled channels over wide ranges of flow parameters. In the viscosity-dominated flow regime, mass transfer is primarily enhanced by steady streaming. In the inertia-dominated flow regime, greater enhancement of mass transfer is

NOMENCLATURE

a	wave amplitude of wavy wall [m]
A	area of mass transfer surface [m^2]
C_b	concentration of the ferricyanide ion [mol m^{-3}]
D	diameter of piston [m]
$\mathscr{D}$	molecular diffusivity of the ferricyanide ion [m^2 s^{-1}]
F	Faraday constant [C mol^{-1}]
f	frequency of oscillation
H_{max}	maximum spacing between walls [m]
i_d	diffusional current [A]
P	oscillatory fraction defined by equation (4), dimensionless
Q_i	instantaneous flow rate [m^3 s^{-1}]
Q_o	peak flow rate of oscillatory component [m^3 s^{-1}]
Q_s	net flow rate [m^3 s^{-1}]
Re_s	Reynolds number defined by equation (3), dimensionless
Re_i	Reynolds number based on instantaneous flow rate [$= Q_i/(Wv)$], dimensionless
s	length of stroke of piston [m]
Sc	Schmidt number ($= v/\mathscr{D}$), dimensionless
Sh	Sherwood number defined by equation (9), dimensionless
St	Strouhal number defined by equation (10), dimensionless
x_o	center-to-peak amplitude of fluid oscillation defined by equation (8) [m]
T	period of oscillation [s]
t	time [s]
W	width of wavy wall [m].

Greek symbols

α^2	Womersley number defined by equation (5), dimensionless
λ	wavelength of wavy wall [m]
v	kinematic viscosity [m^2 s^{-1}].

obtained by rapid fluid mixing, which is produced by the vortex formation/ejection cycle during oscillatory flow.

In a practical mass transfer device, there will be a net flow superimposed on an oscillatory flow. It is important to know how the net flow affects the mass transfer characteristics described above. The present study of pulsatile flow is an extension of the previous study of oscillatory flow [12]. We examined the effect of net flow on the mass transfer characteristics in the wavy-walled channel used in the previous study. No such study appears to have been reported hitherto.

Although not directly related to the present work, there have been several studies on the use of fluid oscillations in straight-walled tubes [13–15]. In particular, Mizushina *et al.* [13] showed experimentally and theoretically the response of mass transfer rates due to oscillatory flow imposed on a steady laminar flow. Gupta *et al.* [15] examined experimentally the enhancement of mass transfer. The mass transfer rates decrease slightly in pulsatile flow with no flow reversal. On the other hand, when flow reversal occurs, the mass transfer rates increase slightly or are equal to those in steady flow, depending on the frequency parameter proposed by Mizushina *et al.* Thus it is concluded that fluid oscillation alone has little effect on heat and mass transfer. This is because the streamlines in laminar flow are always parallel to the walls, even for time-periodic flow, i.e. there is no fluid mixing, as indicated by Howes *et al.* [8]. However, if fluid oscillation is introduced into the systems with separated flow, rapid fluid mixing leads to heat and mass transfer enhancement as described below.

2. EXPERIMENTAL APPARATUS AND PROCEDURE

The experimental investigation was performed using a low-speed sinusoidally modulated flow water-channel, constructed primarily for this project. The apparatus is shown schematically in Fig. 1. The volumetric flow rate is

$$Q_i = Q_s + Q_o \sin(2\pi t/T) \tag{1}$$

where Q_s is the net flow, Q_o is the peak flow of fluid oscillation and T is the period of oscillation.

The net flow is provided by a centrifugal pump and the flow rate is determined with a rotameter. The imposed oscillatory flow is generated by a pulsatile pump, driven by a variable speed motor through a Scotch–Yoke mechanism which allows the length of stroke and frequency of the piston to be changed. The peak flow rate is determined by the following relation:

$$Q_o = 2\pi f s(\pi D^2/4) \tag{2}$$

where f is the frequency of oscillation $1/T$, s is the length of stroke of the piston and D is the diameter of the piston.

The channel consisted of a pair of undulating plates, which form the principal walls. Figure 2 shows the dimensions of the channel. There are 14 furrows in the wall of the channel: each furrow is 14 mm long (λ), 3.5 mm deep ($2a$) and 80 mm wide (W). The minimum and maximum gaps between the upper and lower walls H_{min} and H_{max} are 3 and 10 mm, respectively, and the cross-sectional aspect ratio of the channel based on the minimum gap is 26.7.

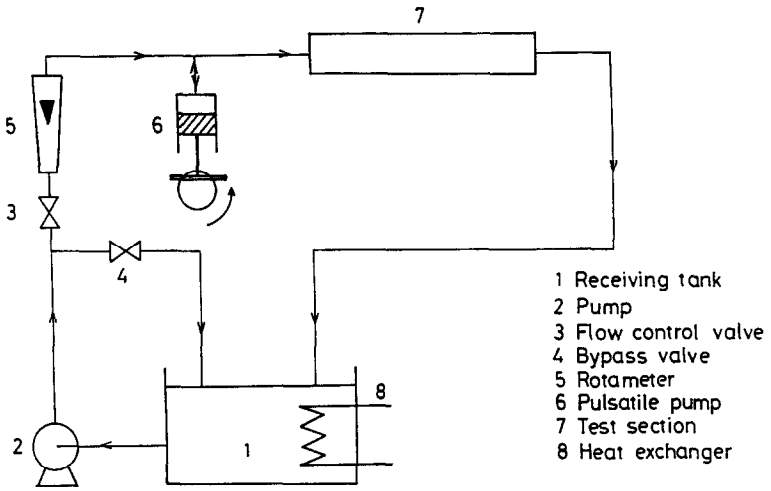

Fig. 1. Flow system.

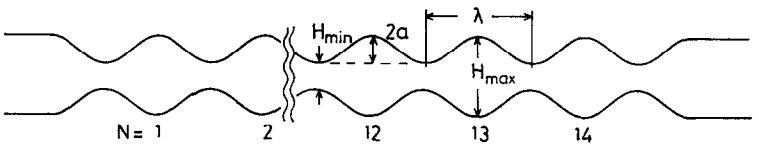

λ =14 mm, 2a=3·5 mm, H_{min} = 3 mm, H_{max}=10 mm, W = 80 mm

Fig. 2. Details of test section.

Three flow parameters characterize pulsatile flow: the net flow Reynolds number

$$Re_s = Q_s/(Wv) \tag{3}$$

the oscillatory fraction of the flow rate

$$P = Q_o/Q_s \tag{4}$$

and the Womersley number

$$\alpha^2 = H_{max}^2(2\pi f)/v. \tag{5}$$

In this study, the following two additional parameters are also employed:

the Strouhal number

$$St = \alpha^2/Re_s \tag{6}$$

and the non-dimensional amplitude of oscillation

$$x_o/H_{max} \tag{7}$$

where v is the kinematic viscosity of the fluid and x_o is the center-to-peak amplitude of fluid oscillation in the channel with a cross-section of $H_{max} \times W$, which is defined by the following equation:

$$x_o = Q_o/(2\pi f H_{max} W). \tag{8}$$

Experiments were carried out in the following ranges of flow parameters: $30 < Re_s < 300$, $0 < P < 17$, $100 < \alpha^2 < 1000$, $0.3 < St < 30$ and $0.153 < x_o/H_{max} < 0.919$. It should be noted that P is determined by Q_s, f and x_o in this experiment. The net flow Reynolds number range belongs to laminar flow [16].

Flow was visualized by means of the aluminum dust method and the electrolytic precipitation method. Perfusion with an aqueous suspension of aluminum particles, about 40 μm in diameter, enabled us to observe pathlines approximately corresponding to streamlines. The electrolytic precipitation method was employed to observe the behavior of fluid mixing for pulsatile flow, its usefulness having been shown for oscillatory flow in a previous study [12]. The smoke of a white metallic compound in water is electrochemically produced from an electroconductive paint on the lower wavy wall and used as a tracer of flow.

The mass transfer rates were obtained by the electrochemical method, which can be applied to unsteady flows [17]. The electrochemical reaction used is the cathodic reduction of ferricyanide ions to ferrocyanide ions at the cathode. The reverse reaction again proceeds at the anode, so that again the bulk concentration of the electroactive species remains unchanged. The reactions occur between the upper and lower walls of the channel. Three cathodes of nickel-plated brass (L/λ = 1, 2 and 3) were used to determine the effect of length of the mass transfer section on the average mass transfer rates. These cathodes were located from the sixth to eighth wave sections in the lower wavy plate, as shown in Fig. 3: the sixth wave section is for $L/\lambda = 1$, the sixth and seventh for $L/\lambda = 2$ and the sixth to eighth for $L/\lambda = 3$. The upper wavy plate, made of nickel-plated brass, served as the anode. The electrolyte used contained 0.01 N potassium ferri–ferrocyanide and 1.0 N sodium

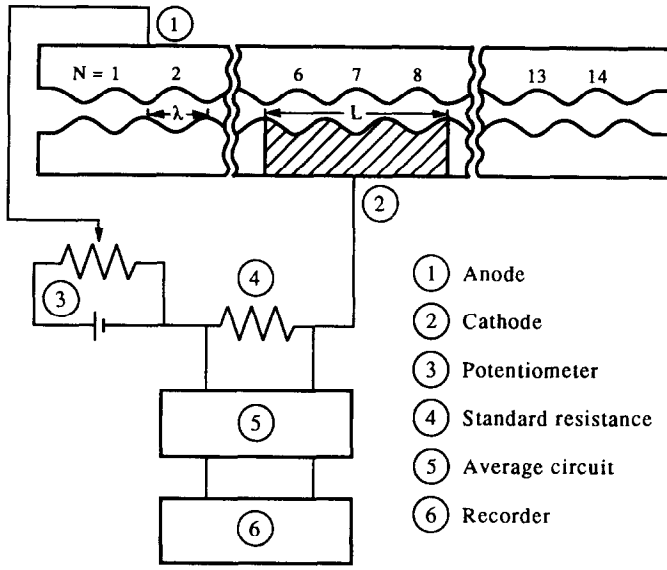

Fig. 3. Positions of electrodes and electrical circuit.

hydroxide, and its temperature was kept at 25°C by a heat exchanger, as shown in Fig. 1 ($Sc = 1570$).

The Sherwood number Sh is related to the diffusional current i_d by

$$Sh = i_d H_{max}/(FC_b A\mathscr{D}) \quad (9)$$

where F is the Faraday constant, C_b is the concentration of ferricyanide ion, A is the area of mass transfer surface and $\mathscr{D}$ is the molecular diffusivity of the ferricyanide ion.

Special care was taken in all experiments to saturate the electrolyte with nitrogen, block off the test section from light exposure and activate the electrodes.

3. EXPERIMENTAL RESULTS AND DISCUSSION

3.1. *Flow patterns and fluid mixing*

The flow patterns which accompany unsteady separation have been described by Nishimura *et al.* [18, 19] and the main features are explained here, together with the behavior of fluid mixing. Figure 4 shows two sets of flow visualization photographs for a small oscillatory fraction of the flow ($Re_s = 100$, $P = 0.29$ and $\alpha^2 = 187$). In the left-hand column, the aluminum dust method represents the streamline patterns. In the other column, the electrolytic precipitation method exhibits the corresponding streakline patterns. The remarkable contrast between the flow observed from a Eulerian perspective (using instantaneous particle paths) and the same flow seen from a Lagrangian viewpoint (using the particle advection trace) is evident for pulsatile flow, unlike steady flow. The nondimensional number Re_i in the figure denotes the Reynolds number based on the instantaneous flow rate Q_i. When the value of Re_i is positive, the flow direction is from left to right, and, if it is negative, the flow direction is reversed. Under this condition, the streamline patterns show the existence of a vortex within each furrow. Although the vortex varies in size with time, it is not displaced from the furrow. Therefore, the streakline patterns change only near the reattachment point, where slight fluid mixing occurs between the mainstream and the furrow. For reference, the streamline and streakline patterns for steady flow are also shown ($Re_s = 100$). Both patterns are identical and fluid is trapped in the vortex, indicating no fluid mixing.

Figure 5 shows the visualization photographs when the oscillatory flow is of the same order as the net flow, and flow reversal occurs ($Re_s = 50$, $P = 1.2$ and $\alpha^2 = 392$). The main features of the streamline patterns are given as follows. The vortex grows during the deceleration phase and eventually disappears during the acceleration phase. During its growth and disappearance, the vortex detaches from the wall and then reattaches due to flow reversal. The streakline patterns vary significantly with time, indicating better fluid mixing between the mainstream and the furrow than with the small oscillatory fraction shown in Fig. 4. Figure 6 shows the visualization photographs of a large oscillatory fraction ($Re_s = 50$, $P = 2.3$ and $\alpha^2 = 188$). The basic flow patterns observed for oscillatory flow remain in pulsatile flow, i.e. a vortex is formed in each furrow, which is ejected in the center of the channel after flow reversal [11, 12]. The streakline patterns become unclear as compared with those in Figs. 4 and 5. This is because fine particles forming streakline patterns diffuse rapidly, indicating a further enhancement of fluid mixing.

Thus, despite the regular laminar flow, rapid fluid mixing between the mainstream and the furrow is observed for a large oscillatory fraction, which is expected to enhance the mass transfer rates.

The features shown in these photographs representing streamline patterns are consistent with the two-dimensional numerical results obtained by a

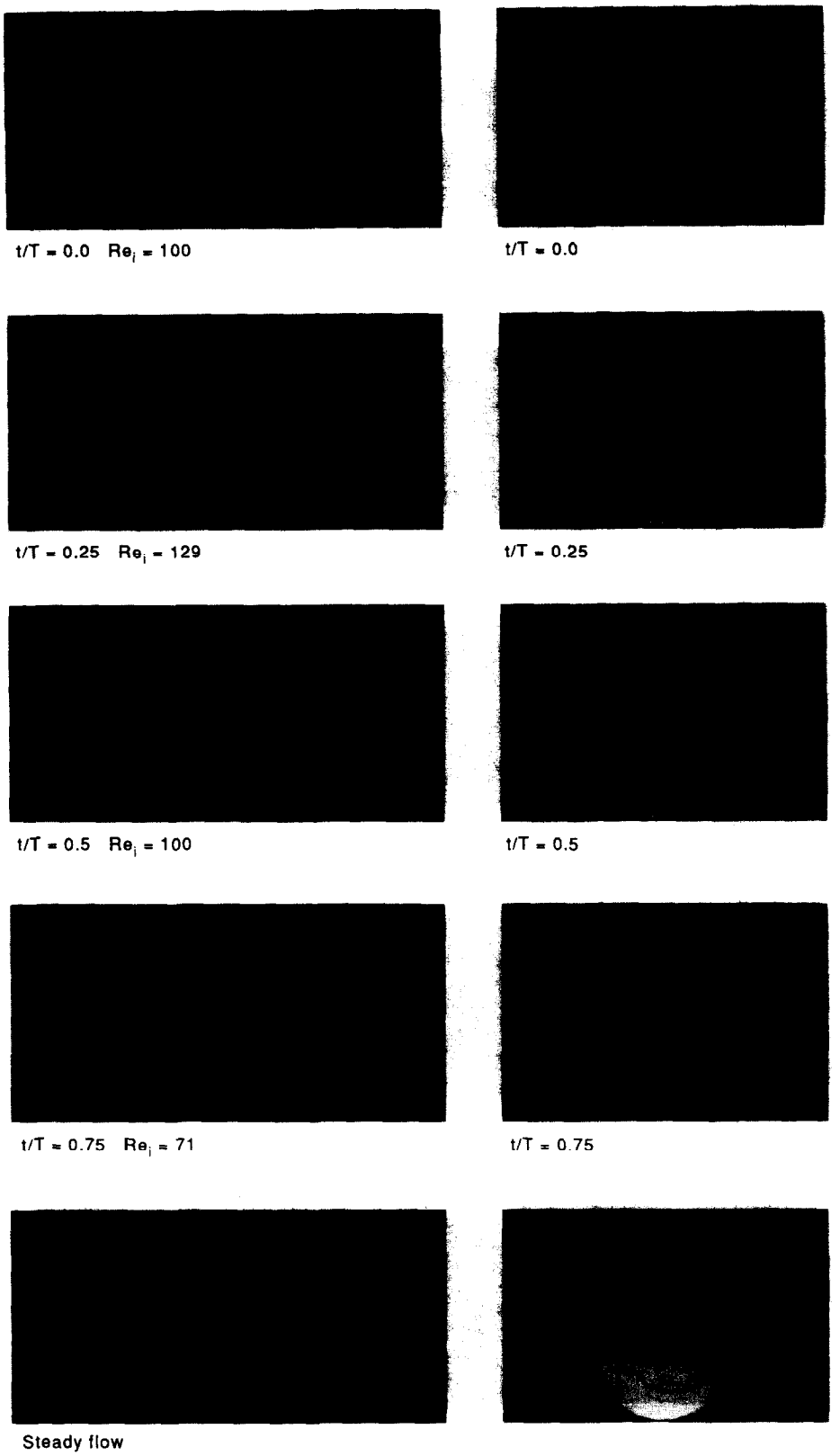

Fig. 4. Flow visualizations by aluminum dust method and electrolytic precipitation method for a small oscillatory fraction of the flow ($Re_s = 100$, $P = 0.29$ and $\alpha^2 = 187$).

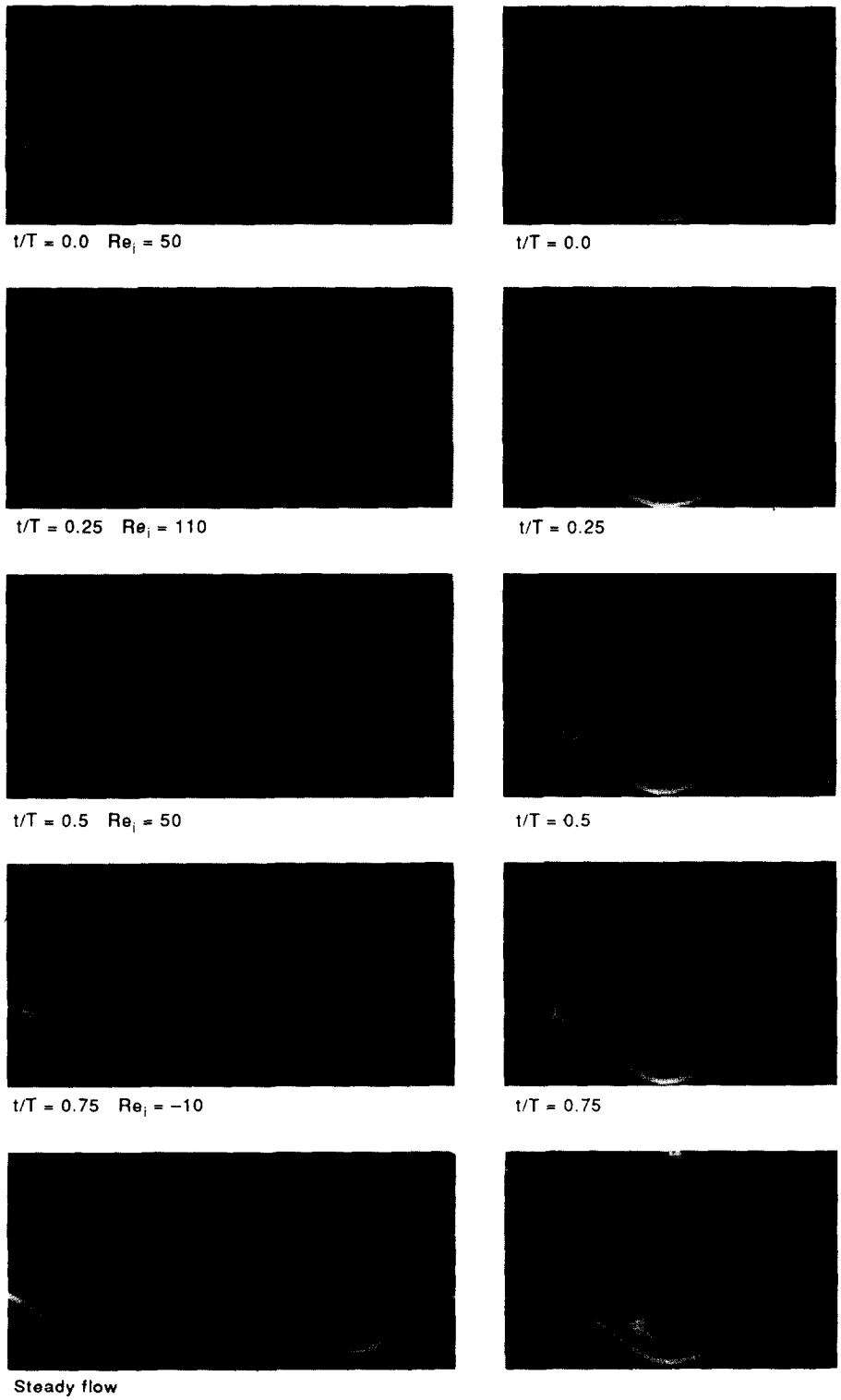

Fig. 5. Flow visualizations when the oscillatory flow is of the same order as the net flow ($Re_s = 50$, $P = 1.2$, $\alpha^2 = 392$).

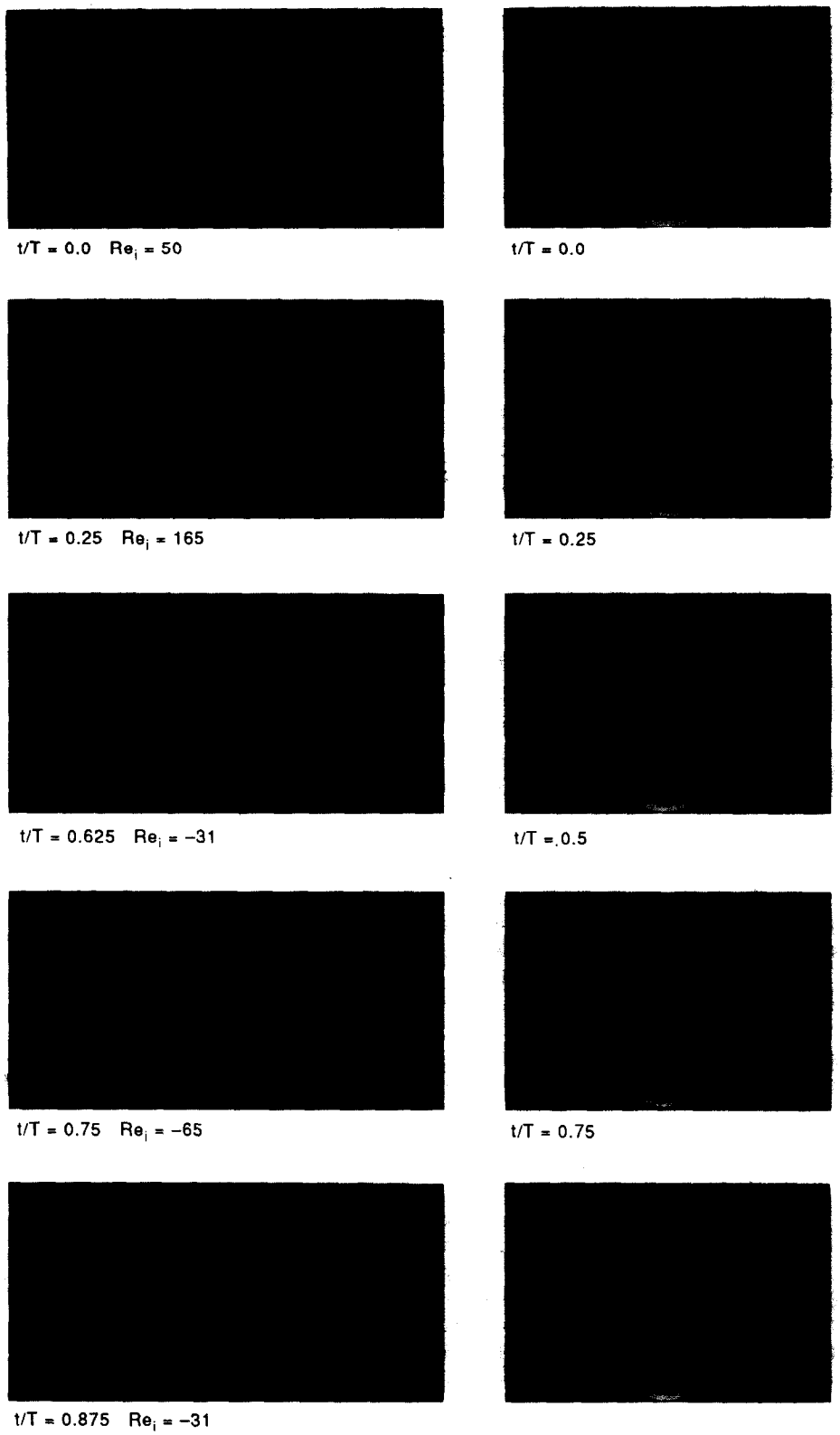

Fig. 6. Flow visualizations for a large oscillatory fraction of the flow ($Re_s = 50$, $P = 2.3$ and $\alpha^2 = 188$).

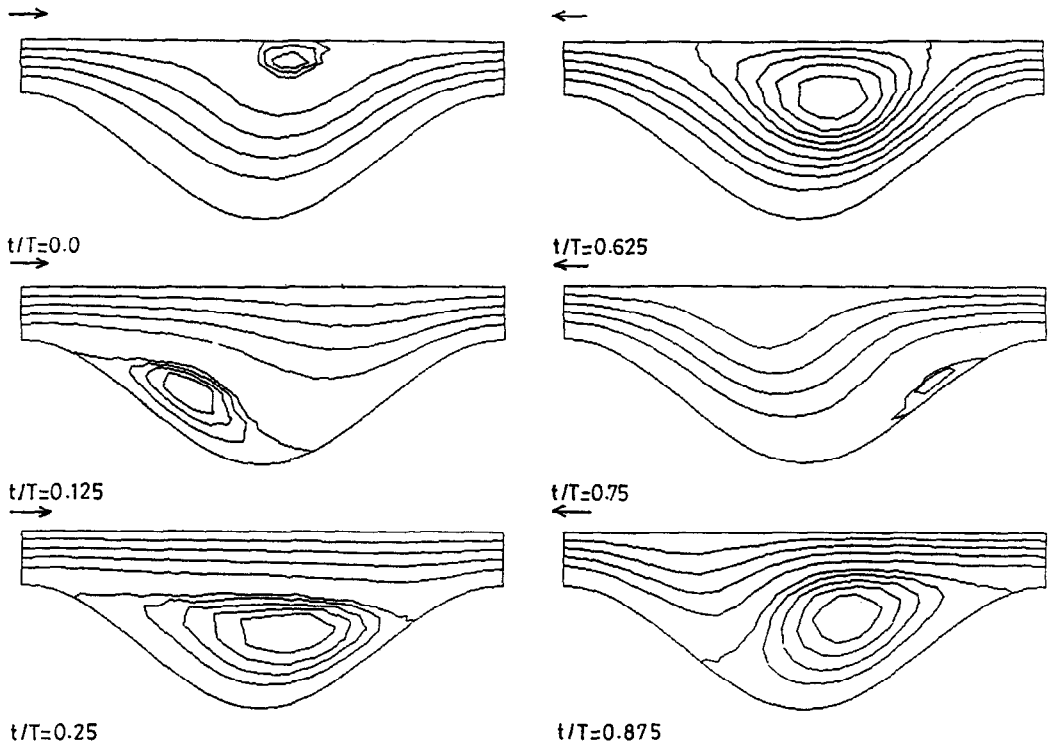

Fig. 7. Computed streamline patterns ($Re_s = 50$, $P = 2.3$ and $\alpha^2 = 188$).

modified version of the finite element method employed previously by Nishimura *et al.* [18]. For example, Fig. 7 shows computed streamline patterns at times in the flow cycle, representing the same conditions as those in Fig. 6. The agreement is satisfactory and the dynamic behavior of the vortex is predicted well. Thus the numerical solutions of the flow field provide a good insight into the details of the time-periodic flow and its quantitative properties, such as wall shear stresses and pressure drop. Figure 8 shows the dimensionless wall shear stress profile corresponding to the streamline patterns of Fig. 7 as an example. Time variation of the wall shear stress is significantly larger at the minimum cross-section $x/\lambda = 0.0$ or 1.0 than at the maximum cross-section $x/\lambda = 0.5$. Although the flow rate at $t/T = 0.0$ is equal to that at $t/T = 0.5$, $t/T = 0.0$ has a larger shear stress than $t/T = 0.5$, and both of them differ from the result for steady flow. This indicates that the flow is not quasi-steady. The time-averaged wall shear stress also shown in the figure is larger than the steady flow value at $Re_s = 50$ and equivalent to that at $Re_s = 150$. This is generated by a nonlinear term in the vorticity transport equation, i.e. a kind of Reynolds stress. Thus this phenomenon is considered to contribute to transport enhancement as well as rapid fluid mixing described above. Furthermore, when the detailed time sequence of the velocity field is known, fluid mixing processes can also be explained numerically by a particle advection procedure in which the same flow is viewed from a Lagrangian rather than from a Eulerian perspective. This is a task for the future.

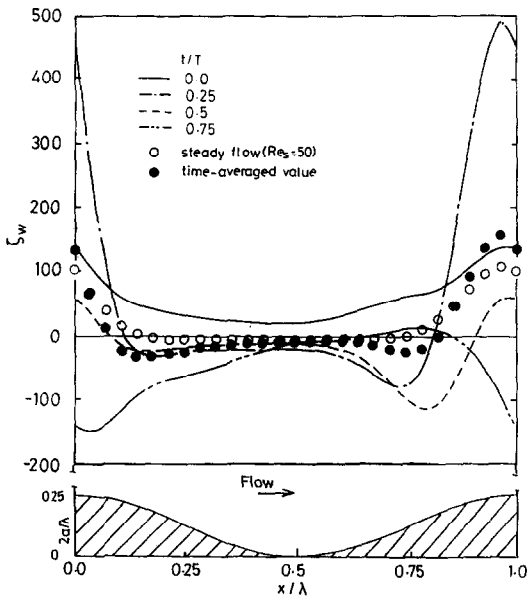

Fig. 8. Computed wall shear stress profiles ($Re_s = 50$, $P = 2.3$ and $\alpha^2 = 188$).

3.2. *Mass transfer*

Although the Sherwood number varies with time, we examine only the time-averaged Sherwood

number, which is an important factor in the design of mass transfer devices. The Sherwood numbers for pulsatile flow are normalized by their steady values to give the mass transfer enhancement factor E. We first describe only the mass transfer results for $L/\lambda = 1$. The effect of mass transfer length is explained later.

Figure 9 shows the relationship between the enhancement factor and the oscillatory fraction of the flow for three different Reynolds numbers. At low Reynolds number ($Re_s = 34$), shown in Fig. 9(a), the enhancement factor E becomes increasingly larger than unity as the oscillatory fraction P increases and

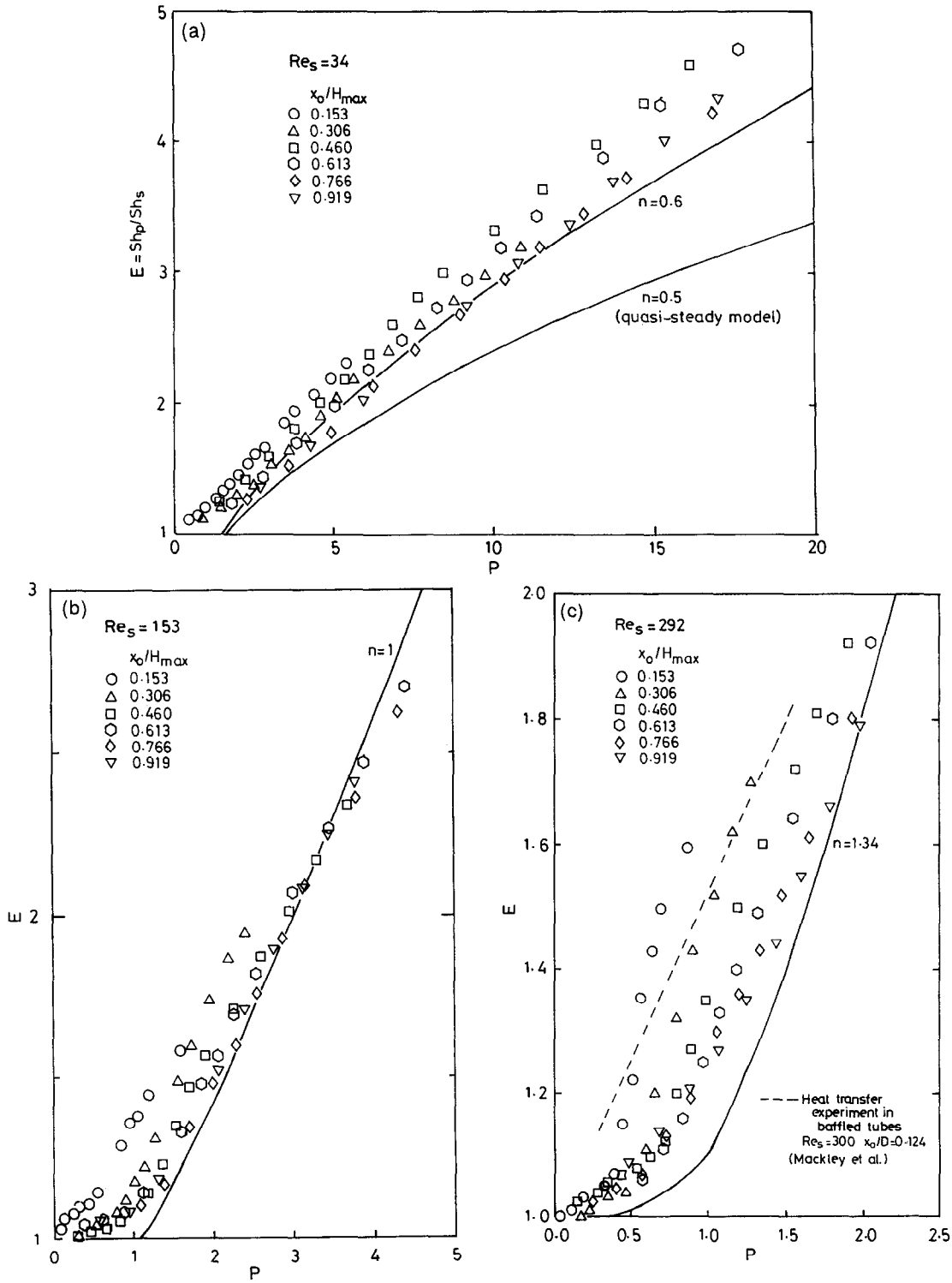

Fig. 9. Enhancement factor vs oscillatory fraction of the flow for $L/\lambda = 1$.

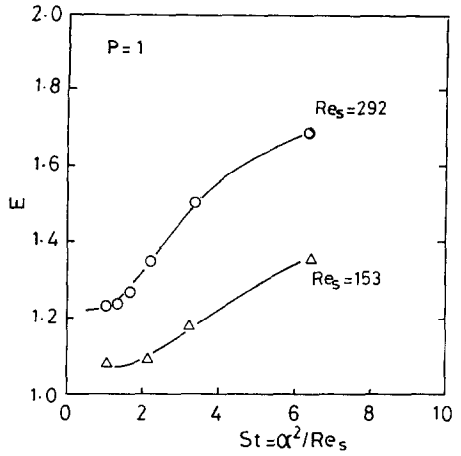

Fig. 10. Enhancement factor vs Strouhal number for $L/\lambda = 1$.

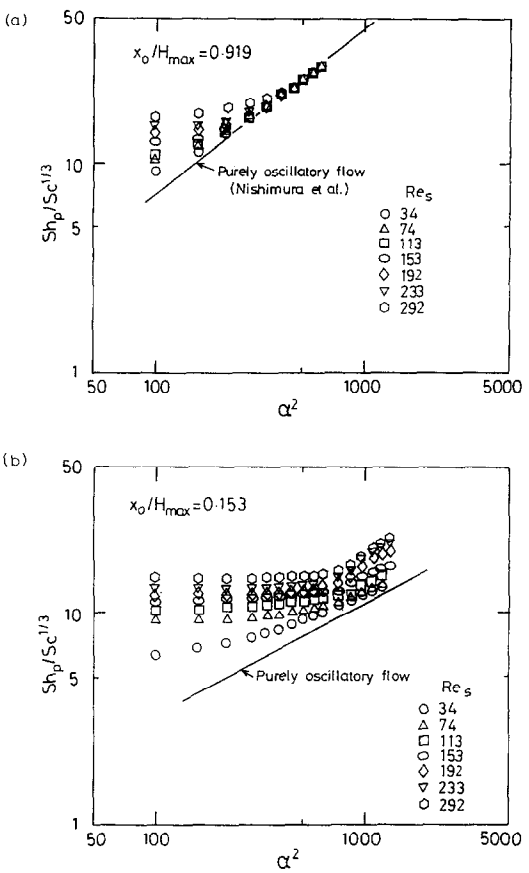

Fig. 11. Comparison of Sherwood numbers for pulsatile and oscillatory flows for $L/\lambda = 1$.

is dependent on the amplitude of fluid oscillation x_o/H_{max}. The solid lines in the figure are estimated by the quasi-steady model [20]. In the quasi-steady model it is assumed that the instantaneous Sherwood number is equal to that of a steady flow, at a flow rate equal to the instantaneous flow rate of the pulsatile flow. Assuming that the Sherwood number is proportional to the n power of the Reynolds number, it follows that

$$E = \frac{1}{T}\int_0^T [1 + P\sin(2\pi t/T)]^n \, dt. \qquad (10)$$

For $n < 1$ this function decreases as the oscillatory fraction increases. However, the instantaneous Sherwood number cannot become negative. Therefore the absolute value of the integral has to be taken. The previous study [16] indicated that the Sherwood number for steady flow is approximately proportional to the 0.5 power of the Reynolds number in the laminar flow range. The experimental data lie above the curve of $n = 0.5$ corresponding to the quasi-steady model. Figure 9(b) and (c) shows the results at higher Reynolds numbers ($Re_s = 153$ and 292). The exponent n represented by the quasi-steady model exceeds unity with increasing Reynolds number, implying increment of the enhancement factor. For reference, the heat transfer experiments of oils in baffled tubes [6] are shown in Fig. 9(c). Although the geometrical conditions are quite different, the behavior of transport enhancement is similar to our results. Also it is noticed that the effect of the amplitude of fluid oscillation becomes more significant as the Reynolds number increases. In other words, this indicates the effect of the frequency of fluid oscillation. Figure 10 shows the relationship between the enhancement factor and the Strouhal number when the oscillatory flow rate is the same as the net flow rate ($P = 1$). In addition to the effect of the oscillatory fraction, the enhancement factor is found to be dependent on the Reynolds number and the Strouhal number.

The above mass transfer results support the idea that transport enhancement is possible by rapid fluid mixing, i.e. combination of flow separation and fluid oscillation.

Next we examine how the mass transfer rates for pulsatile flow are related to those for oscillatory flow. The Sherwood numbers for oscillatory flow have been reported in a previous study [12]. Figure 11 shows a comparison of Sherwood numbers for both flows for two extreme cases ($x_o/H_{max} = 0.919$ and 0.153). For a large amplitude of fluid oscillation shown in Fig. 11(a), as the Womersley number increases the Sherwood numbers become independent of the Reynolds number and asymptotically reach the correlation of oscillatory flow. The result for a small amplitude also reveals a similar trend, as shown in Fig. 11(b). However, it is noted that the Sherwood numbers at higher Reynolds numbers depart from the correlation of oscillatory flow and become larger. To demonstrate the effect of amplitude of fluid oscillation, we replot the experimental data using the following equation:

$$Sh_p^m = Sh_s^m + Sh_o^m \qquad (11)$$

where m is the exponent and subscripts mean s—steady flow, o—oscillatory flow, and p—pulsatile flow.

Figure 12 shows the several results in terms of the groupings in equation (11). Values of the exponent ranging from 2 to 4 have been rationalized, achieving

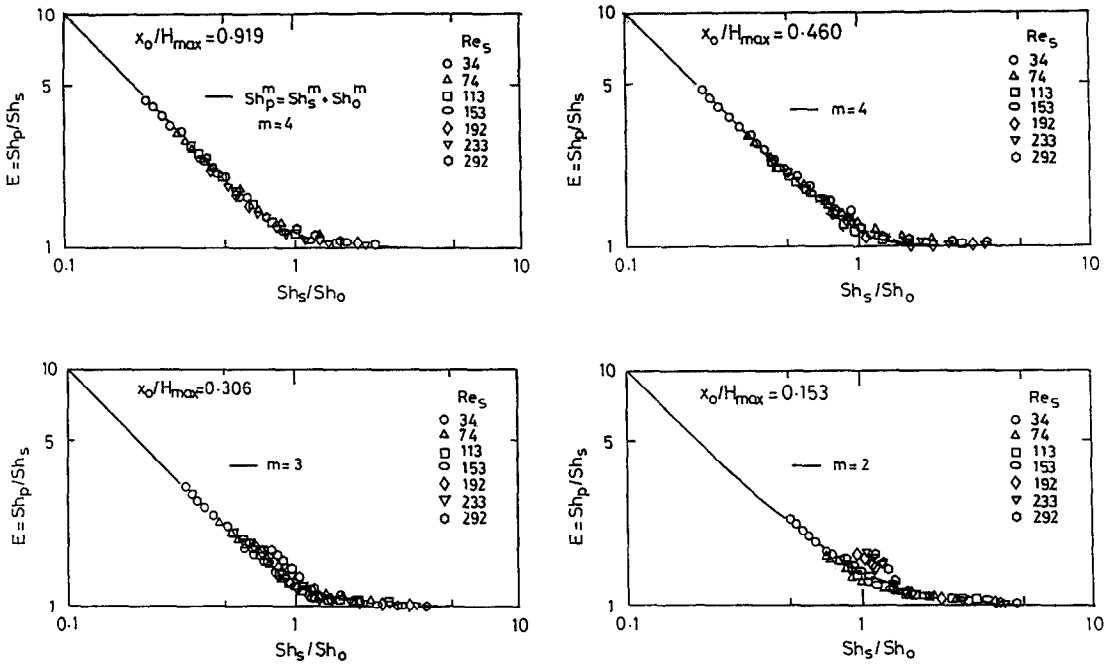

Fig. 12. Relation between Sh_p/Sh_s and Sh_s/Sh_o for $L/\lambda = 1$.

the best fit with experimental data. For $x_o/H_{max} > 0.46$, the exponent has a constant value, $m = 4$, and the relation is independent of Reynolds number. For $x_o/H_{max} < 0.306$, the exponent tends to become smaller as the amplitude of fluid oscillation decreases. This is probably due to the frequency effect. The Sherwood number ratio corresponding to the enhancement factor tends to increase with decreasing amplitude of fluid oscillation, as shown in Fig. 9. This means that, for a given oscillatory fraction of the flow rate, the Sherwood number ratio increases with the frequency of fluid oscillation in this experiment. It is therefore thought that a similar effect appears, especially at small amplitudes, in Fig. 12. In all cases, the oscillatory component is found to contribute to the mass transfer enhancement. Furthermore, the experimental data at high Reynolds numbers depart from each relation. Thus another mechanism appears to operate for mass transfer enhancement at small amplitudes and high Reynolds numbers. As described by Patera and Mikic [4], small fluid oscillations at the natural frequency of the hydrodynamic instability dramatically modulate the flow pattern in a grooved channel, even for Reynolds numbers below the critical value at the onset of self-sustained oscillations, and enhance heat transfer rates. It is expected that a similar phenomenon occurs in the present wavy-walled channel. Figure 13 shows the flow visualization photographs below the critical Reynolds number ($Re_s = 240$, $P = 0.78$ and $\alpha^2 = 391$). Although the imposed frequency is less than the natural frequency of the hydrodynamic instability, the mainstream undulates greatly during the deceleration phase and the flow becomes asymmetric, in contrast to the symmetric flows shown in Figs. 4–6. This is due to a shear layer instability which does not appear at low Reynolds numbers. Detailed study will be performed in the near future.

Finally, we examine the effect of mass transfer length. Figure 14 shows the enhancement factor for three different mass transfer lengths, i.e. $L/\lambda = 1$, 2 and 3. The abscissa in the figure is the imposed frequency instead of the oscillatory fraction, unlike Fig. 9, because the effect of mass transfer length for each Reynolds number is clearly shown in this figure. The effect of mass transfer length appears at low Reynolds numbers and the enhancement factor increases as the value of the mass transfer length increases. This is effective for the enhancement device. However, if the experimental data are plotted using equation (10), the effect of mass transfer length is minute. Figure 15 shows the results for $L/\lambda = 3$, which are apparently identical to those in Fig. 12 for $L/\lambda = 1$.

4. CONCLUSIONS

Our experimental study of flow patterns and mass transfer characteristics in a symmetric sinusoidal wavy-walled channel for pulsatile flow has led to the following conclusions:

(1) Mass transfer rates are always enhanced by a combination of flow separation and fluid oscillation, which leads to rapid fluid mixing. The enhancement factor increases with the oscillatory fraction of the flow. In addition, the Reynolds number and the frequency of fluid oscillation affect the enhancement factor at high Reynolds numbers. In particular, the enhancement of the mass transfer rate increases as the Reynolds number increases in this experimental range.

Fig. 13. Visualizations for asymmetric flow ($Re_s = 240$, $P = 0.78$ and $\alpha^2 = 391$).

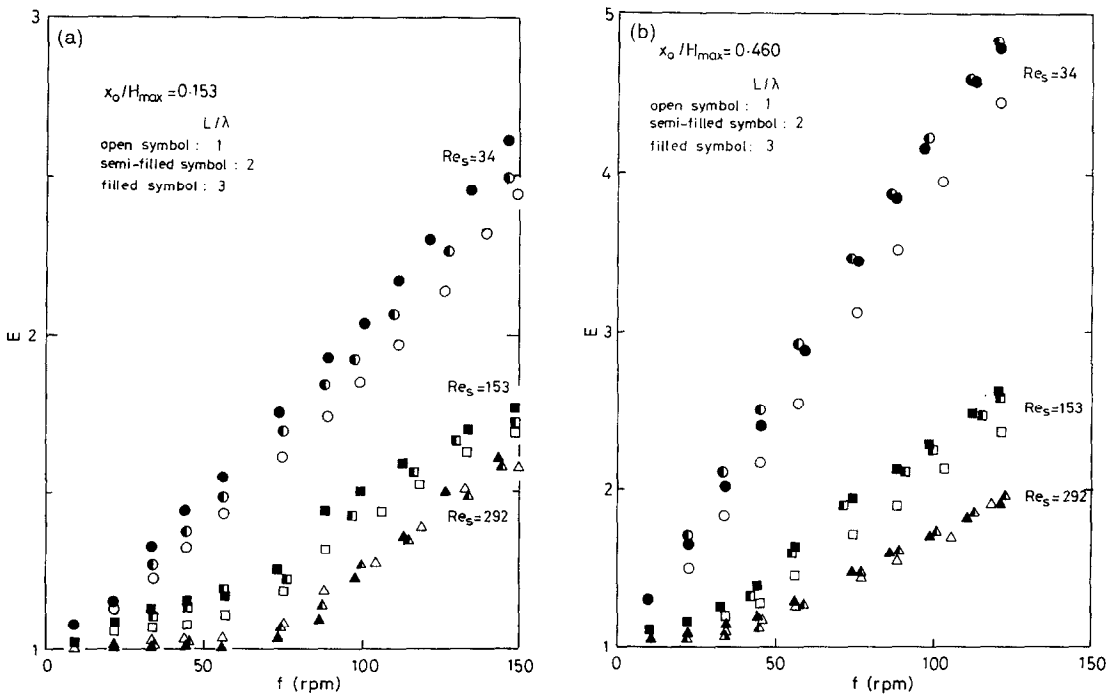

Fig. 14. Enhancement factor vs frequency of fluid oscillation : effect of mass transfer length.

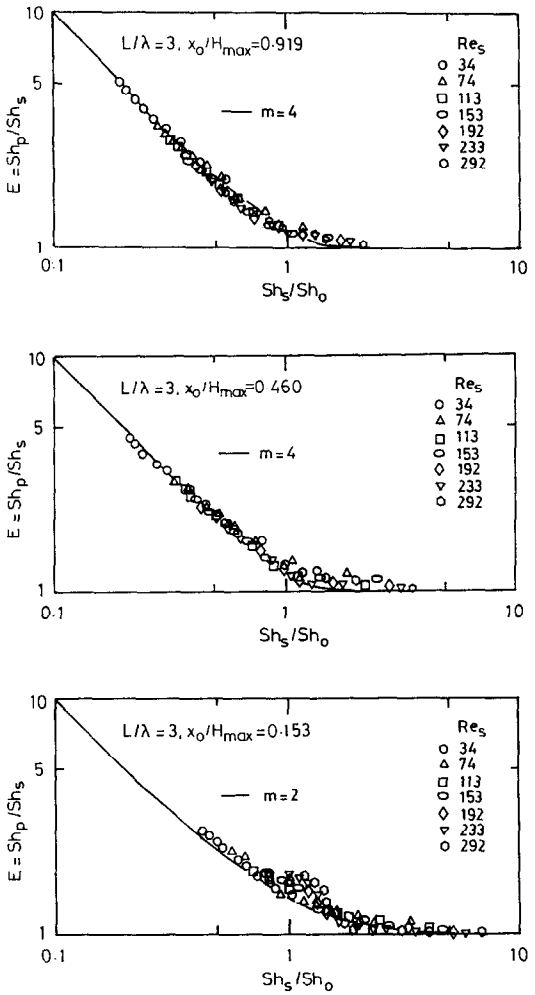

Fig. 15. Relation between Sh_p/Sh_s and Sh_s/Sh_o for $L/\lambda = 3$.

(2) The Sherwood number for pulsatile flow can be expressed by the following relation by superimposing the Sherwood numbers for steady and oscillatory flows:

$$Sh_p^m = Sh_s^m + Sh_o^m.$$

Values of the exponent range from 2 to 4, depending on the amplitude of fluid oscillation, but the exponent at large amplitude is constant, i.e. $m = 4$. At small amplitude and high Reynolds number, the experimental data depart from the above relation, due to the effect of hydrodynamic instability.

Acknowledgements—This work was supported in part by a Grant-in-Aid for Science Research (Nos. 63750899 and 03302031) from the Ministry of Education, Science and Culture of Japan. The authors acknowledge with thanks the assistance of graduate students S. Shimazaki and T. Yano in the experiments.

REFERENCES

1. J. M. Ottino, Mixing, chaotic advection and turbulence, *A. Rev. Fluid Mech.* **22,** 207–255 (1990).
2. H. Aref, Stirring by chaotic advection, *J. Fluid Mech.* **143,** 1–21 (1984).
3. B. J. Bellhouse, F. H. Bellhouse, S. B. MacMurray and J. M. Nelems, A high efficiency membrane oxygenator and pulsatile pumping system and its application to animal trials, *Trans. Am. Soc. Artif. Intern. Organs* **19,** 72–79 (1973).
4. A. T. Patera and B. B. Mikic, Instabilities—resonant heat transfer enhancement, *Int. J. Heat Mass Transfer* **29,** 1127 1138 (1986).
5. M. Greiner, An experimental investigation of resonant heat transfer enhancement in grooved channels, *Int. J. Heat Mass Transfer* **34,** 1384–1391 (1991).
6. M. R. Mackley, G. M. Tweddle and I. D. Wyatt, Experimental heat transfer measurements for pulsatile flow in baffled tubes, *Chem. Engng Sci.* **45,** 1237–1242 (1990).
7. M. R. Mackley and X. Ni, Mixing and dispersion in a baffled tube for steady laminar and pulsatile flow. *Chem. Engng Sci.* **46,** 3139–3151 (1991).
8. T. Howes, M. R. Mackley and E. P. L. Roberts, The simulation of chaotic mixing and dispersion for periodic flows in baffled channels, *Chem. Engng Sci.* **46,** 1669–1677 (1991).
9. T. Nishimura, A. Tarumoto and Y. Kawamura, Flow and mass transfer characteristics in wavy channels for oscillatory flow, *Int. J. Heat Mass Transfer* **30,** 1007–1015 (1987).
10. T. Nishimura, S. Arakawa, S. Murakami and Y. Kawamura, Oscillatory viscous flow in symmetric wavy-walled channels, *Chem. Engng Sci.* **44,** 2137–2148 (1989).
11. T. Nishimura, H. Miyashita, S. Murakami and Y. Kawamura, Oscillatory flow in a symmetric sinusoidal wavy-walled channel at intermediate Strouhal numbers, *Chem. Engng Sci.* **46,** 757–771 (1991).
12. T. Nishimura, S. Murakami and Y. Kawamura, Mass transfer in a symmetric sinusoidal wavy-walled channel for oscillatory flow, *Chem. Engng Sci.* **48,** 1793–1800 (1993).
13. T. Mizushina, T. Maruyama, S. Ide and Y. Mizukami, Dynamic behavior of transfer coefficient in pulsating laminar tube flow, *J. Chem. Engng Jpn* **6,** 152–159 (1973).
14. P. P. Grassmann and M. Tuma, Applications of the electrolytic method—II. Mass transfer within a tube for steady oscillating and pulsating flows, *Int. J. Heat Mass Transfer* **22,** 799–804 (1979).
15. S. K. Gupta, R. D. Patel and R. C. Ackerberg, Wall heat/mass transfer in pulsatile flow. *Chem. Engng Sci.* **37,** 1727–1739 (1982).
16. T. Nishimura, S. Murakami, S. Arakawa and Y. Kawamura, Flow observations and mass transfer characteristics in symmetrical wavy-walled channels at moderate Reynolds numbers for steady flow, *Int. J. Heat Mass Transfer* **33,** 835–845 (1990).
17. T. Mizushina, The electrochemical method in transport phenomena. In *Advances in Heat Transfer* (Edited by T. P. Irvine and J. P. Hartnett), Vol. 7, pp. 87–161. Academic Press, New York (1971).
18. T. Nishimura, T. Yoshino and Y. Kawamura, Numerical flow analysis of pulsatile flow in a channel with symmetric wavy walls at moderate Reynolds numbers, *J. Chem. Engng Jpn* **20,** 479–485 (1987).
19. T. Nishimura and H. Miyashita, Pulsatile flow in a symmetric sinusoidal wavy-walled channel. *Trans JSME, Ser. B* **58,** 1688–1694 (1992).
20. W. Linke and W. Hufschmidt, Wärmeübergang bei pulsierender Stromung. *Chem. Ingr. Tech.* **30,** 159–165 (1954).